



## Studying the Behavior of a Ni-Ti Shape Memory Alloy Wire

Saja M. Abbas<sup>1,\*</sup>, Jamal A.-K. Mohammed<sup>1</sup>, Wisam E. Abdul-Lateef<sup>1</sup>

<sup>1</sup> Electromechanical Eng. Dep., University of Technology, Baghdad, Iraq

### ARTICLE INFO

#### Article history:

Received 20 July 2025

Received in revised form 29 November 2025

Accepted 10 December 2025

Available online 5 January 2026

#### Keywords:

Ni-Ti; SMA wire; experimental tests; strain; stress

### ABSTRACT

Shape memory alloys (SMAs) are a special family of alloys that possess the ability to "remember" their shape and may even return to it when bent. At low temperatures, this alloy may seem to be plastically deformed; but, by increasing the temperature, this "plastic" strain might be repaired. The possession of these distinctive properties made these alloys very important and were widely employed in many technical fields, especially in the robotics, medical, safety and military sectors. This, in turn, encouraged scientists to test these alloys in order to learn more about how they behaved. The study examines the behavior of an 80 cm long and 0.5 mm diameter Ni-Ti SMA wire sample via a series of experimental tests (chemical, mechanical, and electrical). This alloy's composition, as determined by chemical analysis, is 35.05% titanium and 64.95% nickel. The alloy wire's maximum tensile force and extension were 380 N and 10.8 mm, respectively, according to the findings of the mechanical tests; its maximum stress and strain were 1850 MP and 21.7%, respectively. According to the electrical test findings, the wire could support lifting up to 2 kg of weight when 0.2 A of current passed through it.

## 1. Introduction

Shape Memory Alloys (SMAs) are smart materials [1] that, when heated, may take on a predefined shape again. An SMA has a quite low yield strength and may be readily shaped into any new shape that it will hold when it is cold, or below its transformation temperature. On the other hand, the material changes its crystal structure and takes on its previous shape when heated over its transition temperature. The SMA may produce incredibly powerful forces during this change if it meets any opposition.

Due to its special properties [2-4], the SMAs are discovered to offer a great deal of promise for use as actuators [5] in a variety of cutting-edge applications [1]. The unique phase transformation of this alloy makes it important and creates a strong motivation for many researchers to subject it to many tests in order to study its behavior. The evaluation of the thermal properties of two common intelligent system actuators, the SMA helical spring and the Ni-Ti SMA cantilever was presented by Degeratu, *et al.*, [6]. Thermal analysis tests were focused on determining the transition temperatures

Corresponding author

E-mail address: [eme.22.24@grad.uotechnology.edu.iq](mailto:eme.22.24@grad.uotechnology.edu.iq)

<https://doi.org/10.37934/sej.12.1.2434>

and other thermal properties of the two examined actuators. Under a constant or fluctuating load, Saikrishna *et al.*, [7] examined the thermo-mechanical cycle on the SMA wire over the transformation range. Forced cooling and resistive heating were used to complete the cycles. Using a non-contact laser device, the displacement of the wire throughout the thermomechanical cycle was tracked. Throughout the experiment, the recovery strain and the residual deformation were regularly monitored.

Depending on a thorough analysis of electrical resistivity (ER) of a SMA, Zhang *et al.*, [8] suggested a model of self-sensing to accomplish the combined muscle-like tasks of actuating and autonomous-sensing for the built SMA-artificial muscle (AM). To confirm the ER model's validity, a number of thermal, electrical, and mechanical tests are conducted, and under various stress circumstances, the SMA-AM autonomous-sensing function was well proven. Bhargaw *et al.*, [9] described a SMA wire's thermo-electric properties. They discovered that a significant mechanical force is applied to the wire owing to phase transition when it is electrically heated over its transformation point of temperature by a DC current. SMA wire has to be heated and cooled by 0.680 A of current during 796 sec whiles being naturally convection-cooled in order to be used as an actuator. At 43 MPa of stress, 4.33% of the strain was recovered, and the equivalent variation in resistance value was 11.2%. Florian, *et al.*, [10] examined several physical attributes, including thermal, thermomechanical, magnetic, calorimetric, and adhesive capabilities, of a commercially available SMA featuring a rectangular form. Based on the applied pressures, the SMA strip's elasticity range, elasticity–viscoelasticity coexistence area, and domain, which is where a maximal force application of 18 N, were identified.

Sławski *et al.*, [11] investigated at how the electrical resistance of the Ni-Ti alloy (Flexinol) changed under minor elongation cyclic stretching. A specialized test stand was created that included a motorized vertical test stand, an electric resistance measurement equipment, and a force gauge. For the 120 mm long, 0.1 mm Flexinol wire, variations in electrical resistance were examined. The obtained data demonstrated that Flexinol wire's electrical resistance decreases with each stretching cycle. Xiong *et al.*, [12] demonstrated and produced an electro-thermal form memory alloy helical spring actuator made of copper-cored enameled wire and SMA. Through numerical simulation and actual testing, the thermo-mechanical characteristics of the actuator were confirmed. According to the experimental findings, at 100°C, the actuator can generate a peak output displacement of 7.7 mm and a peak recovery force of 70.2N. At a current of 3A, the actuator responds in 26 sec.

In order to monitor the growth of electrical resistivity and the behavior of stress, strain, and temperature in Ni-Ti SMA wires under controlled stress settings, Rodinò *et al.*, [13] designed an automated experimental method. Large-scale datasets were produced, and they show clear stress-dependencies in transformation temperature points, recoverable strain, and electrical resistivity—three important SMA material properties.

The current work is unique compared to the aforementioned previous studies in that it adopts a comprehensive study of all the chemical, mechanical and electrical properties of the alloy by subjecting the alloy to many tests. These tests include chemical analysis testing as well as both electrical and mechanical tests.

## 2. Phase Change Cycle of SMA

Figure (1) depicts the full cycle of the thermo-mechanical change of SMAs [14].

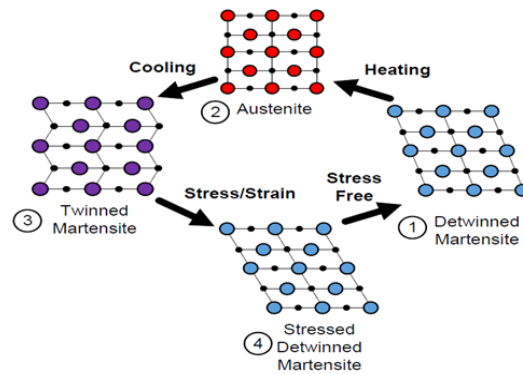


**Fig. 1.** SMA'S Phase change cycle [14]

The bulk material is first thought to start randomly in the non-twinning martensite phase (1). Low yield strength, strain rate, and modulus of elasticity are characteristics of this phase. The alloy is in its greatest extended condition in this configuration. When heated, the alloy undergoes a phase transition that starts at the austenite start temperature, also known as the activation temperature. In an ideal case, the alloy undergoes a continuous transition in the range (0-100 %) austenite (2) across the structure, resulting in a maximum ten percent shrinkage in length overall. At the austenite ending temperature, the phase change is complete. A rise in Young's modulus is also linked to the austenite phase. The opposite change process takes place if the substance cools. At the martensite starting and ending temperatures, the transition from austenite to martensite takes place. A relatively minor change in overall length characterizes the reverse transition, in contrast to the transition from martensite to austenite. The material is in the twinned condition of martensite upon returning to its initial temperature (3). By applying force, which strains the material, the martensite twinning phase may be restored to the non-twinning martensite phase (4).

## 2. Experimental Tests and Results

A SMA wire sample with a length of 80 cm and a diameter of 0.5 mm will be subjected to a series of experimental tests (chemical, mechanical, and electrical) in order to examine its behavior.

### 2.1 Chemical Analysis

It is significant to mention that the chemical composition and structure created during thermomechanical processing determine the combined mechanical qualities that are desired in SMAs. The chemical analysis was conducted at the Department of Applied Sciences - University of Technology by using scanning electron microscopy (SEM) device as shown in Fig. 2a. The chemical analysis test was conducted to find out the percentage of chemical compounds of the SMA wire. The wire is formed in such a way that it is suitable for testing where the rays are directed towards the SMA sample using a device (SEM) as shown in Fig. 2b. The results showed that the chemical compounds that make up the SMA wire are nickel and titanium with atomic mass ratios of 64.95% for nickel and 35.05% for titanium. According to these ratios, the alloy can be regarded as a pure binary system of Ni and Ti. The SMA with different composition will have a great influence on its mechanical properties. It is worth noting the fact that minor compositional modifications can have a significant impact on the alloy's transition temperature. Figure 3 shows a sketch of the percentage of elements contained in the SMA wire and their weight percentages.

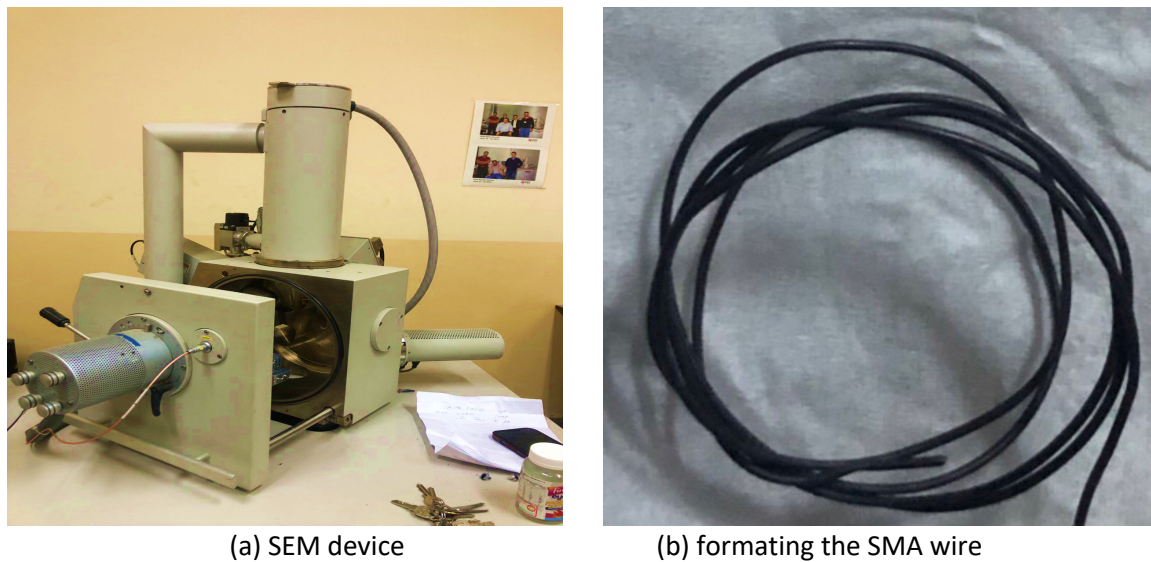
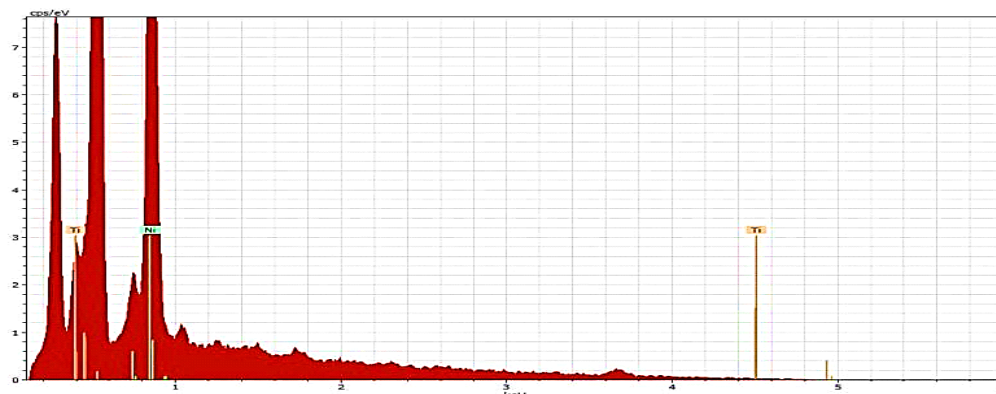


Fig. 2. Chemical analysis

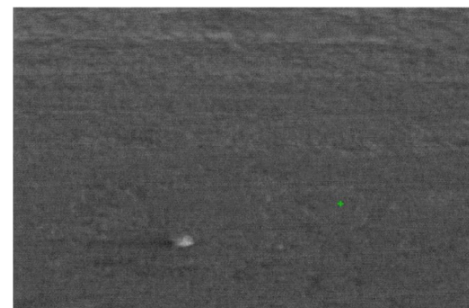


(a) Sketch of Ni & Ti weight percentages

Spectrum: Acquisition 6217

El	AN	Series	Unn. C [ wt. %]	norm. C [ wt. %]	Atom. C [ at. %]	Error	(1sigma) [ wt. %]
Ni	22	L - series	64.95	64.95	69.43		12.24
Ti	28	L - series	35.05	35.05	30.57		5.80
Total:			100.00	100.00	100.00		

(b) Weight percentages for Ni & Ti



(c) SMA under SEM device

Fig. 3. Results of the chemical analysis

## 2.2 Mechanical Tests

Using an Instron machine wdw50 device, the mechanical test (tensile test) was conducted at the Department of Materials Engineering - University of Technology. The wire's maximum tensile force and extension were 0.380 kN and 10.8 mm, respectively, while its maximum stress and strain were 1850 MP and 21.7%, respectively. The tensile test was conducted by inserting 15 cm sample of SAM

wire into an Instron device for 96.5 sec. Figures (4) and (5) show the results of the tensile test on the wire before and after it was performed.

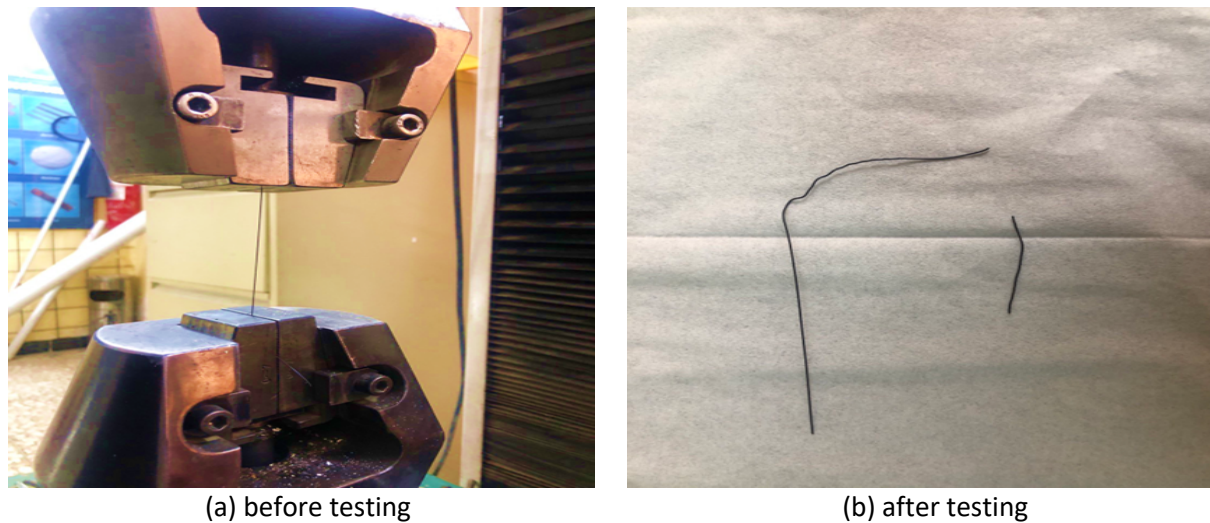


Fig. 4. Mechanical test of SMA wire

The relationship between the SMA wire's stress and strain is seen in Fig. 5. A graphical representation of a material's behavior under increasing loads is called a stress-strain curve. The definition of strain is the ratio of a dimension's changed length to its initial length, whereas the definition of stress is the force to cross-sectional area. It can be seen from the figure that the proposed MSA exhibits exceptional elasticity as well as elevated compressive capacity. These properties are mostly attributed to the plateau area in the stress-strain relationship, which is caused by the transformation phase of stress-induced martensitic. Initially, it was observed that the application of a stress of about 200 MPa, leads to an exacerbated increase in strain until it reaches about 8%, then there is an almost linear direct relationship between stress and strain, continuing until the wire collapses and breaks at a stress value of about 1900 MPa. In general, the increase in strain with stress is governed by the Young's modulus equation as [15]:

$$Young\ modulus = \frac{stress}{strain} \ N/m^2 \quad (1)$$

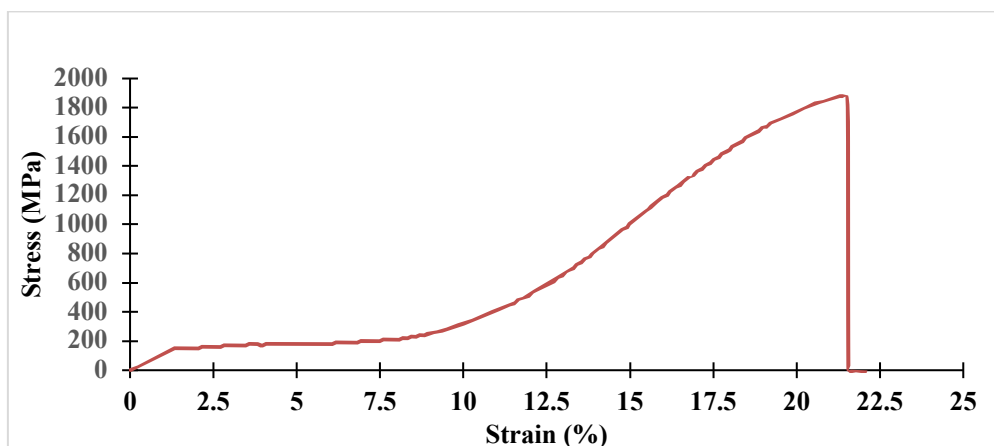


Fig. 5. The strain-stress relationship

Also, the relationship between the tensile force (loading) and the extension that is brought about by this force is seen in Fig. 6. The characteristic in this figure indicates a high load-to-extension ratio (kg / mm). This high ratio leads to superior elasticity which means that large distortions can be readily repaired. The results indicate that the maximum tensile force and extension of the SMA wire reaches up to are 0.380 kN and 10.8 mm, respectively, and that a rise in tensile force also induced an increase in SMA wire extension. Hooke's law [16], which may be used to explain these outcomes:

$$F = K\Delta x \quad (2)$$

Where F is the force applied and it is measured in (N), K is Hooke's constant and it is measured in (N/m), and  $\Delta x$  is extension value in (m).

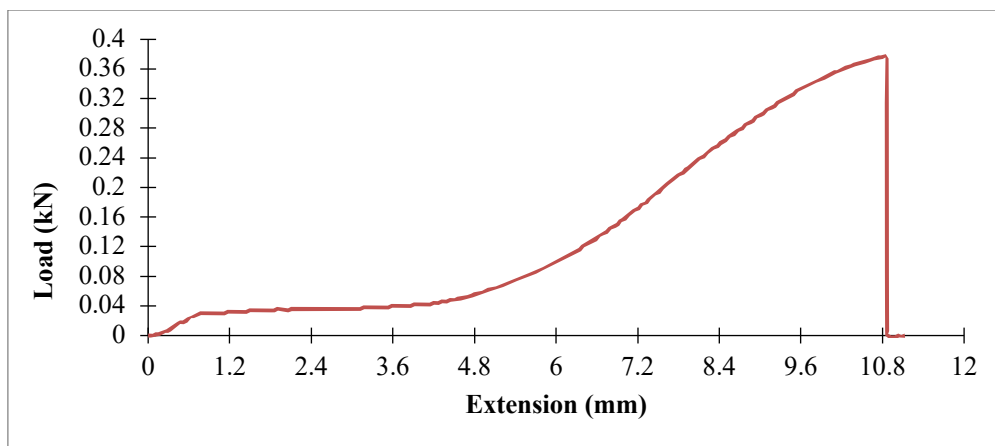


Fig. 6. The Relation between tensile force and strain extension

### 2.3 Electrical Tests

The electrical tests were conducted at the Department of Electromechanical Engineering - University of Technology. The setup arrangement depicted in Figure 7 was utilized to conduct the necessary electrical tests. The setup has an SMA wire of 80cm length and 0.5mm diameter, fixed at one end and left moving on the other side via a pulley to lift different amounts of weight. The electrical testing is carried out using many instruments and measuring devices, including a DC power supply, two digital multimeters (one for measuring voltage across the wire and the other for measuring current flowing through it), thermal resistance to limit the current in the SMA wire, and a thermocouple device for measuring heat released by the wire when it is energized by electric current. During the experiment, the wire is equipped with a DC electric current from the power source ranging between 0.02-0.2 A. Figure 8 shows the electrical circuit wiring diagram used to conduct the required tests.



Fig. 7. Electrical test setup

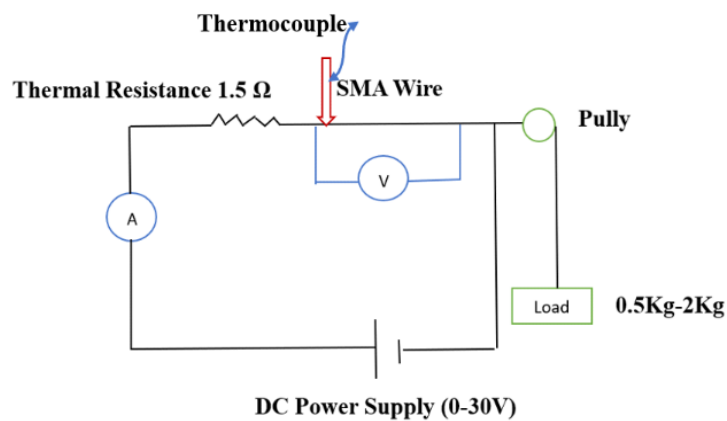


Fig. 8. Schematic of electrical circuit

The measurement of electrical resistance ( $R$ ) is performed by recording the potential difference ( $V$ ) across the alloy wire and the electric current ( $I$ ) passing through it at regular time intervals. The electrical resistance  $R$  is calculated by applying Ohm's law [13]:

$$R = V/I \quad (3)$$

The resistivity  $\rho$  of the wire can be calculated from the relation [13]:

$$\rho = A \times R/L \quad (4)$$

Where  $L$  and  $A$  are the length and cross-sectional area of the wire, respectively.

At first, some tests are frequently implemented to find the characteristics shown in Figures (9-13) of resistivity versus the change of excitation current under different values of weights in the range of (0 - 2kg). The value of the controlled current is allowed to increase from 0.02 to 0.2 A (blue curve) with a step value of 0.02 A and then decrease again from 0.2 A to 0.02 A (orange curve) to study the behavior of electrical resistivity of the SMA wire. Figure 9 shows the relationship between current and wire resistivity at no load. The shape is explained by relying on Equations 3 and 4. The relationship between resistivity and current is an inverse, the higher the value of the current, the lower the

resistance value, and vice versa. This is due to increased heating resulting from increased energy loss ( $I^2R$ ). This decrease in resistance continues until 0.08 A. After that, the resistance is fixed at a certain value due to the constant temperature of the wire after this value and continues to remain stable until 0.2 A. When the current is allowed to return from 0.2 A, the resistance rises to a maximum value at 0.18 A, then decreases until it stabilizes at 0.12 A, and still almost constant until the current decreases to 0.02 A. The same scenario applies almost to the rest of Figures (10-13), when the wire is loaded by different value of weights, but the resistance stability period will be short. It is also noted that increasing the weight value leads to a decrease in the maximum resistivity value. This decrease can be explained by relying on the stress law (Equation 5) as well as resistivity law (Equation 4). Increasing the weight leads to an increase in the stress applied to the wire and thus increase in the wire length. The relationship between force and area is a direct relationship. The greater the weight, the longer the wire, which inversely affects the wire resistivity.

It is also noted from all Figures (9-13) that when the current begins to decrease, the alloy does not return to the same previous resistivity curve as before when it increased. This results from the occurrence of the hysteresis phenomenon, which is characteristic of these alloys. The figures depicting the electrical resistance characteristics of SMA wires demonstrate the alloy's distinctly non-linear and complex behavior, which can be attributed to dynamic changes influenced by various factors, including temperature, martensite reorientation, phase transformation, stress, deformation, and  $r$ -phase distortion.

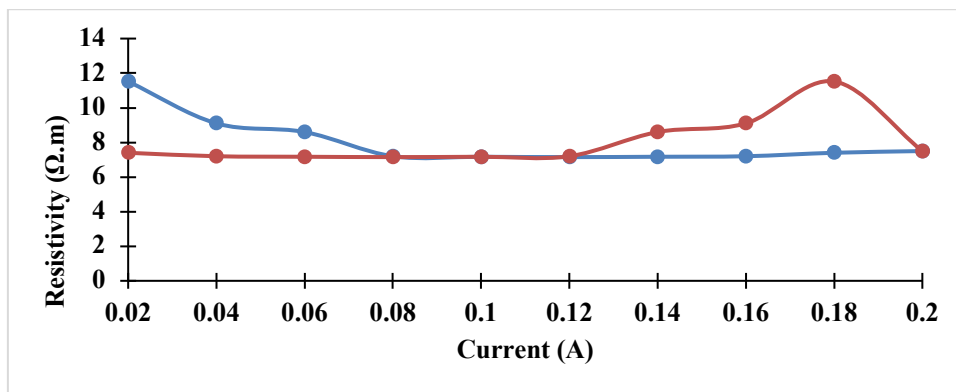


Fig. 9. The relationship between resistivity and current at no load

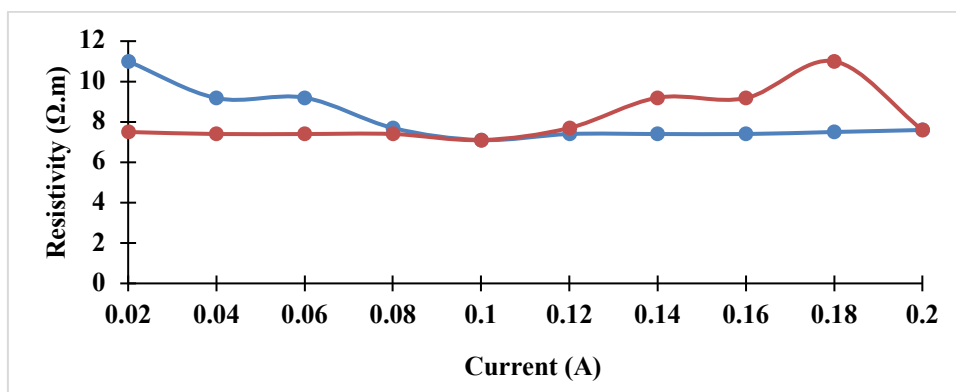


Fig. 10. The relationship between resistivity and current at load of 0.5 kg

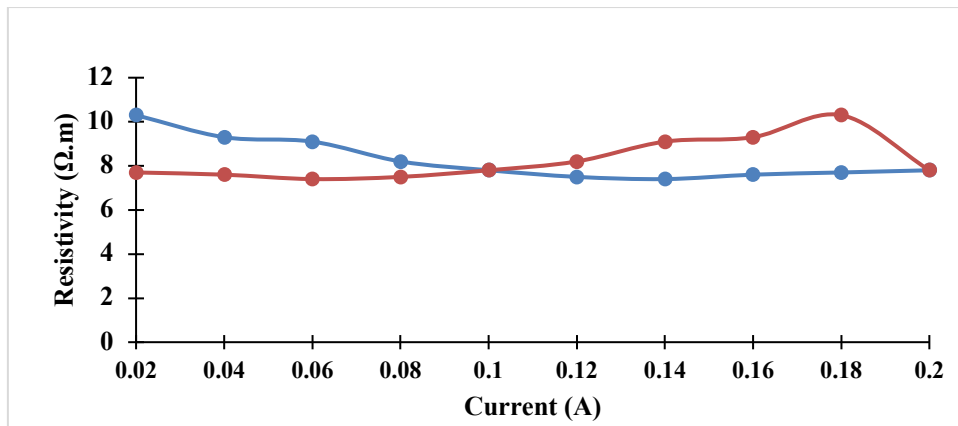


Fig. 11. The relationship between resistivity and current at load of 1 kg

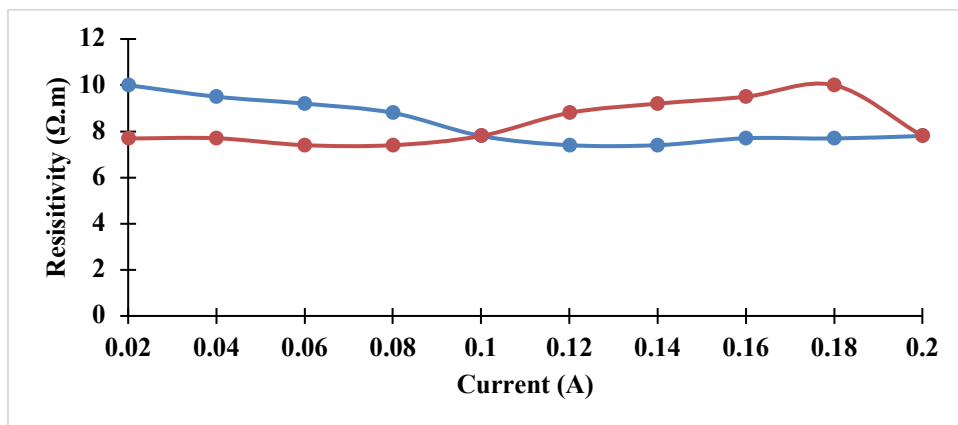


Fig. 12. The relationship between resistivity and current at load of 1.5 kg

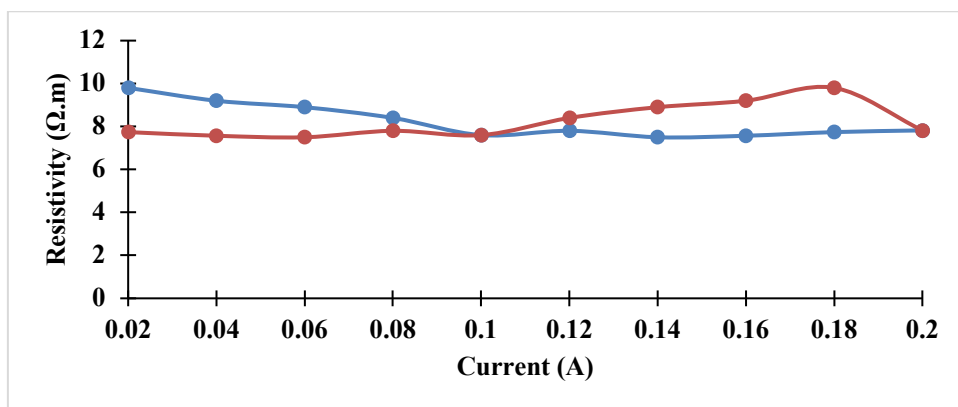


Fig. 13. The Relationship between resistivity and current at load of 2 kg

Figure 14 shows the relationship between the excitation current and temperature at no load. It is noted that the temperature of the wire increases with the increase in the current value from 0.02A until it reaches its maximum value at current of 0.2A, due to the increase in energy loss ( $I^2R$ ). When the current starts to decrease, the relationship is reversed as a result of the phenomenon of hysteresis. Figure 15 shows how the resistance of the wire is inversely proportional to its temperature in the heating state, where the wire resistance decreases until its temperature reaches 31.2 C°, and after this value it stabilizes until the temperature reaches 52.2C°. When the temperature drops again (cooling), the resistance rises again and returns to its previous state before heating occurred.

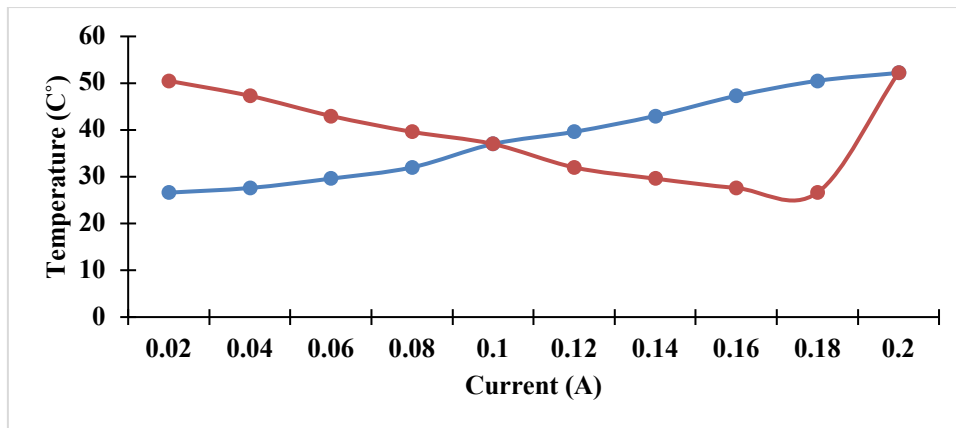


Fig. 14. The relationship between resistance and temperature at no load

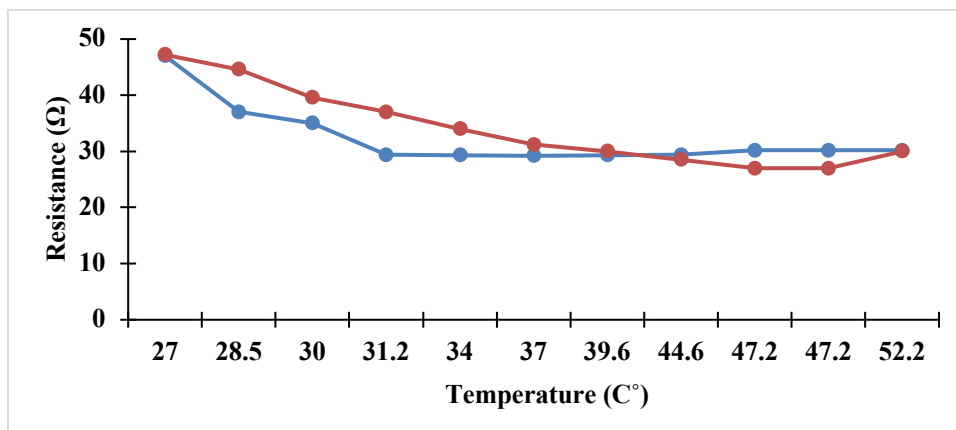


Fig. 15. The relationship between resistance and temperature at no load

### 3. Conclusions

This study examined the behavior of a shape memory alloy wire made of Ni-Ti through a battery of chemical, mechanical, and electrical tests. These tests led to the conclusion that this alloy has unique and intriguing electromechanical properties. The outcomes of the mechanical tests revealed that the alloy wire's maximum tensile force and extension were 0.380 kN and 10.8 mm, respectively, and that its maximum stress and strain were 1850 MP and 21.7%, respectively. According to the electrical test findings, the wire could support up to 2 kg of weight when 0.2 A of current was run through it. This alloy can pass current with a density of up to 101.86 A/cm<sup>2</sup> and measures 80 cm long and 0.5 mm in diameter. According to the test findings, the Ni-Ti alloy exhibits good extensibility and can be easily current-controlled to create relatively high force and displacement in the SMA by heating, which qualifies it for use as an actuator in a variety of applications.

### Acknowledgements

My sincere appreciation goes out to the research supervisors, Dr. J.A.-K. Mohamed and Dr. W.E. Abdul-Lateef, for their direction, fervent support, and helpful critique of this study.

### References

- [1] Shukla, Uddeshya, and Kamal Garg. "Journey of smart material from composite to shape memory alloy (SMA), characterization and their applications-A review." *Smart Materials in Medicine* 4 (2023): 227-242. <https://doi.org/10.1016/j.smim.2022.10.002>

- [2] Al-Hassani, Emad S., M. Sahib Al-Saffar, and A. Zena. "Preparation and Characterization of Biomedical Ni-Co-Al Shape Memory Alloys." *Eng. & Tech. Journal* 34. <https://doi.org/10.30684/etj.34.7A.17>
- [3] Abbass, Muna Khethier, Munther Mohamed Al-Kubaisy, and Raad Suhail Ahmed Adnan. "The effect of thermo-mechanical treatment on mechanical properties & microstructure for (Cu-Al-Ni) shape memory alloy." *Engineering and Technology Journal part (A) Engineering* 34, no. 13 (2016): 2518-2526. <https://doi.org/10.30684/etj.34.13A.14>
- [4] Al-Hassani, E. S., A. H. Ali, and S. T. Hatem. "Investigation of corrosion behavior for copper-based shape memory alloys in different media." *Engineering and Technology Journal* 35, no. 6 Part A (2017): 578-586.. <https://doi.org/10.30684/etj.35.6A.4>
- [5] Kim, Min-Soo, Jae-Kyung Heo, Hugo Rodrigue, Hyun-Taek Lee, Salvador Pané, Min-Woo Han, and Sung-Hoon Ahn. "Shape memory alloy (SMA) actuators: The role of material, form, and scaling effects." *Advanced Materials* 35, no. 33 (2023): 2208517. <https://doi.org/10.1002/adma.202208517>
- [6] Degeratu, Sonia, P. Rotaru, Gh Manolea, H. Manolea, and A. Rotaru. "Thermal characteristics of Ni-Ti SMA (shape memory alloy) actuators." *Journal of thermal analysis and calorimetry* 97, no. 2 (2009): 695-700. <https://doi.org/10.1007/s10973-009-0215-0>
- [7] Saikrishna, C. N., K. V. Ramaiah, S. Allam Prabhu, and S. K. Bhaumik. "On stability of NiTi wire during thermo-mechanical cycling." *Bulletin of Materials Science* 32, no. 3 (2009): 343-352. <https://doi.org/10.1007/s12034-009-0049-1>
- [8] Zhang, Jian-Jun, Yue-Hong Yin, and Jian-Ying Zhu. "Electrical resistivity-based study of self-sensing properties for shape memory alloy-actuated artificial muscle." *Sensors* 13, no. 10 (2013): 12958-12974. <https://doi.org/10.3390/s131012958>
- [9] Bhargaw, H. N., M. Ahmed, and P. Sinha. "Thermo-electric behaviour of NiTi shape memory alloy." *Transactions of Nonferrous Metals Society of China* 23, no. 8 (2013): 2329-2335. [https://doi.org/10.1016/S1003-6326\(13\)62737-5](https://doi.org/10.1016/S1003-6326(13)62737-5)
- [10] Florian, Gabriel, Augusta Raluca Gabor, Cristian-Andi Nicolae, Andrei Rotaru, Cornelia A. Marinescu, Gabriela Iacobescu, N. Stănică, Sonia Degeratu, Oana Gîngu, and Petre Rotaru. "Physical and thermophysical properties of a commercial Ni-Ti shape memory alloy strip." *Journal of Thermal Analysis and Calorimetry* 138, no. 3 (2019): 2103-2122.). <https://doi.org/10.1007/s10973-019-08615-9>
- [11] Sławski, Sebastian, Marek Kciuk, and Wojciech Klein. "Assessment of SMA electrical resistance change during cyclic stretching with small elongation." *Sensors* 21, no. 20 (2021): 6804. <https://doi.org/10.3390/s21206804>
- [12] Xiong, Yang, Jin Huang, and Ruizhi Shu. "Thermomechanical performance analysis and experiment of electrothermal shape memory alloy helical spring actuator." *Advances in Mechanical Engineering* 13, no. 10 (2021): 16878140211044651. <https://doi.org/10.1177/16878140211044651>
- [13] Rodinò, S., M. Siciliano, E. M. Curcio, F. Lamonaca, D. L. Carnì, G. Carbone, and C. Maletta. "Development of an automated experimental system for thermomechanical and electrical characterization of NiTi shape memory alloys." *Experimental Mechanics* 64, no. 3 (2024): 425-440. <https://doi.org/10.1007/s11340-024-01036-2>
- [14] Wright, Cody Alexander. *Thermo-mechanical system identification of a shape memory alloy actuated mechanism*. Old Dominion University, 2016. <https://doi.org/10.25777/meap-ct77>
- [15] Choren, John Anthony, Stephen M. Heinrich, and M. Barbara Silver-Thorn. "Young's modulus and volume porosity relationships for additive manufacturing applications." *Journal of materials science* 48, no. 15 (2013): 5103-5112. <https://doi.org/10.1007/s10853-013-7237-5>
- [16] Giuliadori, Mauricio J., Heidi L. Lujan, Whitney S. Briggs, Gurunanthan Palani, and Stephen E. DiCarlo. "Hooke's law: applications of a recurring principle." *Advances in physiology education* 33, no. 4 (2009): 293-296. <https://doi.org/10.1152/advan.00045.2009>